The corticothalamocortical circuit drives higher-order cortex in the mouse

Brian B. Theyel[1], **Daniel A. Llano**[2], and **S. Murray Sherman**[1]

[1] Department of Neurobiology, University of Chicago, Chicago, IL 60637, USA

[2] Department of Neurology, University of Chicago Medical Center, Chicago, IL 60637, USA.

SUMMARY

An unresolved question in neuroscience relates to the extent to which corticothalamocortical circuits emanating from layer 5B play a role in information transfer through the cortical hierarchy. Here, using a novel form of optical imaging in a brain slice preparation, we demonstrate that the corticothalamocortical pathway drives robust activity in higher-order somatosensory cortex. When the direct corticocortical pathway was interrupted, secondary somatosensory cortex showed robust activity in response to stimulation of the barrel field in primary somatosensory cortex (S1BF), which was eliminated after subsequently cutting the somatosensory thalamus, suggesting a highly efficacious corticothalamocortical circuit. Further, after chemically inhibiting the thalamus, activation in secondary somatosensory cortex was eliminated, with a subsequent return after washout. Finally, stimulation of layer 5B in S1BF, and not layer 6, drove corticothalamocortical activation. These findings suggest that the corticothalamocortical circuit is a physiologically viable candidate for information transfer to higher-order cortical areas.

Much of neocortex can be divided into macroscopic zones: visual, auditory and somatomotor. Each of these is comprised of a number of discrete areas[1-3] that function together to analyze relevant information (e.g., visual, etc.). A key first step towards understanding how cortex functions is to elucidate how information flows between these discrete cortical areas. The prevailing dogma[4-6] is that this flow of information is subserved by direct corticocortical pathways. In the visual system, for example, this implies that once visual information reaches primary visual cortex from the lateral geniculate nucleus, it remains exclusively within cortex as it flows up the cortical hierarchy. In this scheme, beyond relaying the initial information to cortex (e.g., the geniculocortical pathway), the thalamus plays no obvious role beyond modulation of corticocortical information flow[6]. However, a recent hypothesis suggests that much, and perhaps the vast majority, of

information flow between cortical areas involves higher order thalamic nuclei in the form of corticothalamocortical circuits[7-9].

This latter hypothesis is based partly on the idea that many brain circuits can be divided into "drivers", which represent the main information routes and "modulators", which serve to modulate information flow[10, 11]. Well-documented examples of drivers are the retinal input to the lateral geniculate nucleus or lemniscal input to the ventral posterior nucleus; modulator examples are feedback layer 6 corticothalamic projections and cholinergic brainstem inputs to thalamus[10-14]. In this context, the information route involving driver corticothalamocortical circuits emanates from layer 5B cells initiating a feedforward thalamocortical circuit [1, 12], as opposed to the modulating, feedback layer 6 corticothalamic pathway. Though the aforementioned pieces of evidence, in aggregate, are suggestive of a highly efficacious corticothalamocortical circuit, no study has directly tested its ability to activate cortex. We provide evidence here, based on activity of circuits evoked in slices of the mouse brain, that a corticothalamocortical circuit starting in primary somatosensory (barrel) cortex (S1BF) strongly activates secondary somatosensory cortex. This finding suggests that corticothalamocortical pathways are powerful enough to carry receptive-field defining information to higher order cortical areas.

RESULTS

The mouse thalamocortical somatosensory slice[2] contains much of the somatosensory corticothalamocortical circuit (see Fig. 1). The relevant structures in the slice include S1BF, secondary somatosensory cortex, POm and the connections between S1BF/POm and secondary somatosensory cortex/POm[1, 2, 15-17]. To anatomically verify this connectivity, we placed a retrograde tracer (DiI) into the upper layers (layers 2/3 and 4) of secondary somatosensory cortex in the same type of slice used for our experiments. Retrogradely labelled cells were observed in POm, anatomically confirming that at least some of these connections remained. We primarily employed flavoprotein autofluorescence imaging[18, 19] to assess whether the corticothalamocortical circuit can drive secondary somatosensory cortex responses.

Cut Sequence

After verifying flavoprotein autofluorescence activity in both secondary somatosensory cortex and thalamus following electrical stimulation of layer 5B in S1BF, we identified the border between S1BF and secondary somatosensory cortex by locating the abrupt disappearance of barrels, which were visible under both brightfield and fluorescence illumination. We confirmed that this was the correct location by using an atlas and nearby characteristic landmarks[20]. We then used a bent syringe needle to make a radial cut between the stimulation site in S1BF and secondary somatosensory cortex that extended into the white matter, thereby severing the direct corticocortical afferents connecting them (see Methods). After making the cut, we stimulated S1BF at the same location we used for the first stimulus. In 3 slices, activity in secondary somatosensory cortex and POm remained despite ablation of the direct corticocortical pathway (see Fig. 2 and Supplementary Video 2 online for a representative example).   F/F slightly decreased in secondary somatosensory

cortex in all 3 slices and was not significantly different in POm compared to activity levels prior to this cut. We then made a second cut across the dorsolateral aspect of VPm and POm, ensuring the disruption of all thalamic projections to secondary somatosensory cortex (Fig. 2c). S1BF stimulation following this cut failed to activate secondary somatosensory cortex in all 3 slices. To ensure that the cut eliminated any possibility of activating secondary somatosensory cortex, we increased the stimulus amplitude by a factor of 6 during one of our experiments and were still unable to get any appreciable secondary somatosensory cortex activity after the second cut.

These data suggest that direct corticocortical projections are not necessary to activate secondary somatosensory cortex in these slices, and that a corticothalamocortical circuit is capable of doing so. Several other circuits could conceivably be responsible for this activation following direct corticocortical disruption. It is possible that branched collaterals of thalamic relay cell axons that innervate both S1BF and secondary somatosensory cortex[21] were antidromically activated leading to orthrodromic thalamocortical activation of secondary somatosensory cortex. Another possibility is that the cut may not have completely severed corticocortical axons. Finally, an unknown pathway could be involved.

Reversible Inhibition

To ensure that corticothalamocortical circuit activation accounted for our results we employed glutamate stimulation methods, which avoid antidromic activation of (branched) thalamocortical axons. To selectively and reversibly inhibit the corticothalamocortical circuit we focally injected an AMPA receptor blocker, 500 μM 6,7 -dinitroquinoxaline -2,3-dione (DNQX), into the thalamus (see Methods, Fig. 3 below and Supplementary Videos 2 and 3 online). We performed these experiments in 9 slices, each from a different animal, and the results are summarized in Fig. 3d. The maximal secondary somatosensory cortex F/F values decreased by 89.8 +/− 4.5% during runs with maximal thalamic inactivation (n = 9, p = 0.0007, paired t-test). Furthermore, F/F values after DNQX washout were not significantly different from baseline (n = 9, p = 0.33, paired t-test), indicating a full recovery in secondary somatosensory cortex. These data suggest that the corticothalamocortical pathway is a potent activator of secondary somatosensory cortex.

To determine whether the DNQX injection reached S1BF or secondary somatosensory cortex, which could have directly inhibited secondary somatosensory cortex activation, we injected a fluorescent tracer (Texas Red® 10,000 MW lysine-fixable dextran, Invitrogen) into the thalamus using the same protocol we use to inject DNQX (see Fig. 3f and Supplementary Video 3 online). We monitored an entire 6 minute injection to ensure that the injection medium did not reach cortex. It was clear from the video that the injection stream did not approach S1BF or secondary somatosensory cortex. A further indication that the DNQX did not affect the relevant parts of cortex was the stability of upper layer activation in the column we stimulated (see Fig. 3).

During three of the runs, we recorded from a single neuron in the upper layers of secondary somatosensory cortex using whole-cell patch clamp throughout the entire manipulation, providing electrophysiological verification of the imaging results (see Fig. 4). Recordings from each of these three cells and the corresponding flavoprotein autofluorescence signals

were well-aligned with one another, as was expected given the previously-described correlations between flavoprotein autofluorescence signal strength in the neocortex and underlying physiological activity[22]. Before applying DNQX to the thalamus, there was a strong optical signal in secondary somatosensory cortex following S1BF stimulation and a correspondingly robust inward synaptic current in a neuron recorded within the region of the flavoprotein autofluorescence response. After DNQX application, both the optical and electrophysiological signals were abolished, and both returned after subsequent washout of DNQX. Cellular activity, similar to the aforementioned flavoprotein autofluorescence imaging results, decreased by 91.73 +/− 0.47% during successful DNQX trials for the 3 cells, each from separate experiments (n = 3, p = 0.000026, paired t-test). We lost one cell while removing the DNQX pipette, but the remaining two cells regained much of their previous activation. Similar to statistical data for the optical analyses, above, single-cell activity returned to baseline levels after wash for these cells.

Corticothalamocortical Circuit Verification

We sought to ensure that activation in our slices originated in layer 5B, the layer of origin for the corticothalamocortical circuit, and not layer 6, which sends feedback to thalamus. We thus pressure injected glutamate into S1BF in somatosensory slices from two animals starting in layer 5B and steadily moved the stimulation site towards the white matter until the corticothalamocortical circuit was no longer activated. We found that stimulation of layer 6, which sends modulatory afferents to thalamus [10], [12], did not activate secondary somatosensory cortex via this circuit. Subsequent stimuli in layer 5B elicited secondary somatosensory cortex activation, verifying that the circuit was still viable after the failures of the layer 6 stimulations. This sequence was also done in a slice from another animal with low levels of electrical stimulation (2 µA; see Methods for stimulus train parameters); similar results were obtained.

To confirm that stimulation in S1BF was generating suprathreshold activity in the thalamus, we recorded extracellularly from six POm neurons in three somatosensory slices (two neurons each) in a loose seal configuration while photostimulating in S1BF. We observed spiking activity in 2/6 cells from a single slice with an average of 3.64 +/− 0.49 spikes elicited per stimulus (see Supplementary Fig. 1a). We also used extracellular recording electrodes in open configuration (described in Methods) to record multiunit activity from POm in three other slices. We saw reliable multiunit spiking activity that was time-locked to stimulation in S1BF in each slice; see Supplementary Fig. 1b. These data demonstrate that glutamate stimulation in the corticothalamocortical slices we used was able to drive spiking in POm, a requisite for corticothalamocortical circuit activation. Furthermore, when photostimulating in layer 6 of S1BF with the same stimulus both neurons in the loose seal configuration failed to spike, also suggesting that layer 5B, and not layer 6, corticothalamic afferents were responsible for the activation of the corticothalamocortical pathway in our slice preparations.

DISCUSSION

Previous work indicates that individual elements within the corticothalamocortical circuit have driver properties. Layer 5B inputs to POm are of large diameter and contact proximal dendrites, and have synaptic properties consistent with driver inputs[12, 23]. In addition, receptive fields in POm depend on S1BF input[24]. Furthermore, activation of the higher order thalamocortical projection from POm to secondary somatosensory cortex elicits synaptic responses characteristic of driver input[1]. Here we have demonstrated the efficacy of the entire circuit by providing evidence that a substantial proportion of the secondary somatosensory cortex activation our slices depended on thalamic circuitry. Given that our results came from experiments on a brain slice with many cut connections, it is likely that the corticothalamocortical circuit is highly efficacious in an intact animal, though this will need verification.

Our results thus show, for the first time, that a corticothalamocortical circuit involving POm provides a strong connection between S1BF and secondary somatosensory cortex. A question that remains unresolved in our data is the efficacy of the direct S1BF to secondary somatosensory cortex pathway. While we failed to find much evidence regarding the strength of this pathway, we believe that this may be an artifact of our slice, which has been optimized for thalamocortical and corticothalamic circuits. Indeed, other evidence[15] indicates that direct corticocortical connections are mostly cut in this preparation. Thus we emphasize that what we have shown here is a strong, hitherto unexplored, corticothalamocortical circuit, and that is the main point of this investigation. A proper comparison with the direct S1 to secondary somatosensory cortex circuit must await further study.

Before the hypothesis that much of the information transfer between cortical areas involves corticothalamocortical circuits can be accepted, the findings from this study will need to be generalized to other sensory systems *in vitro* (if possible) and *in vivo*. We should note that there is evidence supporting the existence of multiple key features of corticothalamocortical driving circuitry in the visual and auditory systems, including driver-like corticothalamic inputs from layer 5B[25-31], higher order thalamic receptive field dependency on cortical inputs[24, 32] and non-reciprocal corticothalamocortical organization for layer 5B but not layer 6 corticothalamic outputs[33-35]. The presence of similar circuitry in other sensory systems, in combination with the results presented here, suggests that corticothalamocortical information transfer may represent a key addition to, or even replacement of, the current dogma that corticocortical transfer of primary information exclusively involves direct corticocortical pathways.

The corticothalamocortical hypothesis also raises key questions about the utility of thalamic circuitry in information processing. Just as there is no *a priori* reason for information to pass through the thalamus from the sensory periphery to the cortex, there is no obvious reason for an additional thalamic pathway between cortical areas. Further, the presence of corticothalamocortical driving pathways leaves open the question of the nature of the ubiquitous direct corticocortical pathways: are they modulatory, driving, a combination of the two, or something else entirely? While this will require further study, the possibility or

even likelihood that these direct corticocortical pathways do indeed provide another route of information flow would suggest a system of two parallel streams of information: corticocortical and corticothalamocortical. A major difference between these routes might be related to the observation that, while essentially all direct corticocortical projections lie strictly within cortex, the corticothalamocortical pathway emanates from layer 5B cells, most or all of which have axons that branch to innervate thalamus as well as other subcortical structures that appear to be mostly motor in nature[36-38]. Thus, this arm of information transfer reflects output that is sent to both cortical and extrathalamic subcortical motor targets, implying that this circuit, by having a large impact on its cortical target, may be an effective monitor of motor control signals[39].

METHODS

We obtained somatosensory slices[2] from male and female mice (BALB/c *mus musculus*, 12–22 d) using standard, previously published techniques[1] with only minor variations. All procedures were approved by the Institutional Animal Care and Use Committee at the University of Chicago. We first anesthetized the mice (Harlan Sprague-Dawley, Indianapolis, IN) with a mixture of 1 mg/kg ketamine (Vetaket, Phoenix Scientific, Inc., St. Joseph, MO) and 10 mg/kg xylazine , and after the hindlimb reflex was absent, we perfused them with chilled (~4° C) sucrose-based slicing solution[1] prior to cutting. After cutting, we transferred the slices to a holding chamber containing oxygenated artificial cerebrospinal fluid (ACSF), composed of, in mM: NaHCO3 26, KCl 2.5, glucose 10, NaCl 126, NaH2PO4*H2O 1.25, MgCl2*6H2O 3, CaCl2*2H2O 1.1, where they incubated for at least 1 hour prior to imaging/recording.

We implemented whole-cell patch clamp recordings (Fig. 4) using standard, previously described techniques [3], [12], [40-42]. We monitored the access resistance of the cells throughout the recordings, which lasted > 1 hour for most experiments, and only included neurons with a stable access of less than 30MΩ in our analysis.

We performed extracellular recordings presented in Results and Supplementary Fig. 1 (online) in either a loose seal or open configuration. For loose seal recordings, we placed 4–6 MΩ glass pipettes filled with ACSF adjacent to a neuronal cell membrane and applied a slight amount of negative pressure to achieve ~500 MΩ to 1 GΩ for recordings. In open configuration we lowered broken back glass electrodes (~5–10 μm) ~50–100 μm into the tissue (POm). To detect spikes we used manual thresholding in Clampfit (Molecular Devices, Toronto) and used the resulting spike times to construct peristimulus time histograms in Microsoft Excel. We set thresholds well above baseline noise conditions and visually confirmed that the waveforms were consistent with that of an action potential.

We were able to easily identify POm in slices as a thalamic region that had a lighter appearance than the neighboring VPm under brightfield illumination; we distinguished S1BF from secondary somatosensory cortex by the barrels and septa that were resolved in the former. We identified the approximate borders between cortical layers in S1BF (and often in secondary somatosensory cortex) using the following criteria: layer 4 contained characteristic barrel structures and a relative dark contrast compared to layer 5A, which

appeared as a light-color band under brightfield illumination; we were also able to differentiate layer 5B from the neighboring layer 5A and layer 6, even at low magnification, by the presence of a large number of loosely-packed large cell bodies which formed a dark strip under brightfield illumination.

Thalamic Inhibition

For irreversible circuit inactivation (Fig. 3), we placed radial cuts with a bent syringe needle (27 ½ guage) attached to a micromanipulator between S1 and secondary somatosensory cortex, extending through the subcortical white matter to eliminate the direct corticocortical pathway. We then made another cut between VPm and the thalamic reticular nucleus to sever fibers between POm and cortex, thus eliminating the corticothalamocortical circuit. We waited at least 30 minutes after each cut to assess slice activity. For reversible thalamic inactivation, we focally injected ~15 μL 500 μM DNQX in ACSF using a glass micropipette (5–10 μm) over the course of ~7 minutes into an area just adjacent to the thalamic hotspot to avoid damaging relevant thalamic relay cells. We used this method to locally deactivate the circuit without directly affecting cortical activity. The sequence of steps for these experiments proceeded as follows. First, we assessed circuit activation in each slice by microspritzing glutamate or photostimulating via photolysis of glutamate (see Methods) in layer 5B of S1BF. After we saw activation in both POm and secondary somatosensory cortex, we locally applied 500 μM 6,7 -dinitroquinoxaline -2,3-dione (DNQX) to the thalamic hotspot with a micropipette (~5–10 μm diameter) over the course of 6–7 minutes. After applying the DNQX, we stimulated the circuit once every two minutes. If two or more failures of secondary somatosensory cortex activation (assessed by visual inspection of F/F data) occurred followed by return of circuit activation within 20 minutes of the DNQX application, we deemed the run a successful deactivation and subsequent reactivation of the corticothalamocortical circuit.

Stimulation

For the electrical stimulation experiment (Fig. 2) we delivered 20 Hz, 1 second long trains of 10 ms pulses at varying amplitudes before and after each cut using a glass pipette (5–10 μm diameter) filled with ACSF. We delivered a 30 μA stimulus for the baseline run and for the cortical cut run. After the thalamic cut we used a 150 μA train to further illustrate that secondary somatosensory cortex was no longer being activated. During reversible experiments, we used photostimulation (1 experiment) and pressure injection of glutamate (8 experiments). The photostimulation techniques have been previously described[40], [43]. We delivered a 20 Hz, 200 ms long train of 10 ms pulses at 60 mA laser power to Layer 5B of S1BF or injected glutamate using a 20 Hz, 1 second long train of 10 ms pulses at ~4–6 psi using a glass pipette filled with 10 μM L-glutamate in ACSF. We stimulated before DNQX application, then after DNQX application at 2 minute intervals until secondary somatosensory cortex signal elimination and subsequent recovery. If obvious secondary somatosensory cortex deactivation was not achieved, we stopped collecting data 20 minutes after DNQX application. We used our previously described methods for photostimulation[40]-[42]. In past experiments we and others[43], [44] have seen no change of the recording quality or large tissue response changes during photostimulation experiments that might suggest damage from phototoxicity.

Flavoprotein Autofluorescence Imaging

We performed flavoprotein autofluorescence imaging (Figs. 2–4) as previously described[22]. We captured green light (520–560 nm) generated by mitochondrial flavoproteins in the presence of blue light (472–488 nm), using a high sensitivity camera (QImaging Retiga-SRV; QImaging Corporation, Surrey, BC Canada) with a Firewire interface. We acquired all images using 4×4 binning at 8-bits with 2.5x magnification. Final image resolution was 348 × 260 pixels, with 60 pixels spanning 1 mm in both the x- and y- dimensions. We suspended slices above the chamber bottom with a piece of titanium mesh mounted on a hand-bent platinum wire to maintain adequate slice oxygenation and perfusion on both sides of the slice. This has been shown by others[19], and in our experience, to significantly increase the flavoprotein autofluorescence signal amplitude. We typically captured images for 14 second-long sweeps, with stimuli during the second second of each sweep. We stored the resulting images on a custom-built computer running a commercially available software package (Streampix 3; Norpix, Inc., Montreal, Quebec, Canada) and analyzed them with programs that we generated in-house made to run on Matlab. In the case of simultaneous whole-cell recordings (Fig. 4), we selected a box of pixels located immediately over the group of cells near the electrode tip in ImageJ and exported them to Excel, where we produced line graphs.

We typically acquired flavoprotein autofluorescence images at a rate of 7–12 frames per second. We manually adjusted exposure times to yield image brightness (i.e., baseline flavoprotein autofluorescence) that was subjectively similar across experiments. For Figs. 2 and 3: after acquisition and processing (details above), we uniformly adjusted the contrast, brightness and transparency of flavoprotein autofluorescence images and then overlaid onto raw images from Streampix 3 in CorelDRAW X4 (Corel Corporation, Ottawa, Ontario Canada). We added all drawn items (arrows, axes, drawings etc.) with CorelDRAW for Figs. 1–3. We generated Fig. 4 was in Microsoft Excel 2003, then exported to CorelDRAW for font modification and standardization.

Statistics

Descriptive measures throughout the paper are in the form of mean +/− standard error. We used a two-tailed t-test to determine the significance of the DNQX runs (Fig. 3). We obtained data making up the "baseline" condition by using maximal F/F values for baseline runs, runs after DNQX application and runs after we washed out DNQX by selecting a 5×5 pixel box over layer 4 in secondary somatosensory cortex in ImageJ (NIH) and subtracting another set of F/F values obtained from a 5×5 pixel in an area in which we observed no activity (the same method was used in the cut experiment). This helped control for photobleaching and uniform noise. We analyzed runs with the maximal decrease in F/F after DNQX application for the "post-DNQX" condition in each experiment.

We translated whole-cell recording data (currents) presented in Results and Fig. 4 into area (pA*ms) for 2.5 second windows beginning at the stimulus onset. The post-DNQX run and wash run were normalized to the baseline condition for each experiment and were compared using paired t-tests.

Supplementary Material

Refer to Web version on PubMed Central for supplementary material.

Acknowledgements

REFERENCES

1. Lee CC, Sherman SM. Synaptic Properties of Thalamic and Intracortical Inputs to Layer 4 of the First- and Higher-Order Cortical Areas in the Auditory and Somatosensory Systems. J Neurophysiol. 2008; 100:317–326. [PubMed: 18436628]

2. Agmon A, Connors BW. Thalamocortical responses of mouse somatosensory (barrel) cortexin vitro. Neuroscience. 1991; 41:365–379. [PubMed: 1870696]

3. Cox CL, Sherman SM. Control of Dendritic Outputs of Inhibitory Interneurons in the Lateral Geniculate Nucleus. Neuron. 2000; 27:597–610. [PubMed: 11055441]

4. Kaas JH. The Organization of Neocortex in Mammals: Implications for Theories of Brain Function. Annual Review of Psychology. 1987; 38:129–151.

5. Van Essen DC, Anderson CH, Felleman DJ. Information Processing in the Primate Visual System: An Integrated Systems Perspective. Science. 1992; 255:419–423. [PubMed: 1734518]

6. Olshausen BA, Anderson CH, Van Essen DC. A neurobiological model of visual attention and invariant pattern recognition based on dynamic routing of information. J. Neurosci. 1993; 13:4700–4719. [PubMed: 8229193]

7. Sherman SM, Guillery RW. The role of the thalamus in the flow of information to the cortex. Philosophical Transactions of the Royal Society B: Biological Sciences. 2002; 357:1695–1708.

8. Guillery RW, Sherman SM. Thalamic Relay Functions and Their Role in Corticocortical Communication: Generalizations from the Visual System. Neuron. 2002; 33:163–175. [PubMed: 11804565]

9. Sherman SM. Thalamic relay functions. Prog Brain Res. 2001; 134:51–69. [PubMed: 11702563]

10. Sherman SM, Guillery RW. On the actions that one nerve cell can have on another: Distinguishing drivers from modulators. Proceedings of the National Academy of Sciences of the United States of America. 1998; 95:7121–7126. [PubMed: 9618549]

11. Sherman SM, Guillery RW. Functional organization of thalamocortical relays. J Neurophysiol. 1996; 76:1367–1395. [PubMed: 8890259]

12. Reichova I, Sherman SM. Somatosensory Corticothalamic Projections: Distinguishing Drivers From Modulators. J Neurophysiol. 2004; 92:2185–2197. [PubMed: 15140908]

13. Wilson JR, Friedlander MJ, Sherman SM. Fine structural morphology of identified X- and Y-cells in the cat's lateral geniculate nucleus. Proc R Soc Lond B Biol Sci. 1984; 221:411–436. [PubMed: 6146984]

14. Sherman, S. Murray R.W.G. Exploring the thalamus and its role in cortical function. The MIT Press; Cambridge, MA: 2006.

15. Staiger JF, Kötter R, Zilles K, Luhmann HJ. Connectivity in the somatosensory cortex of the adolescent rat: an in vitro biocytin study. Anatomy and Embryology. 1999; 199:357–365. [PubMed: 10195309]

16. MacLean JN, Fenstermaker V, Watson BO, Yuste R. A visual thalamocortical slice. Nat Meth. 2006; 3:129–134.

17. Cruikshank SJ, Rose HJ, Metherate R. Auditory Thalamocortical Synaptic Transmission In Vitro. J Neurophysiol. 2002; 87:361–384. [PubMed: 11784756]

18. Reinert KC, Dunbar RL, Gao W, Chen G, Ebner TJ. Flavoprotein Autofluorescence Imaging of Neuronal Activation in the Cerebellar Cortex In Vivo. J Neurophysiol. 2004; 92:199–211. [PubMed: 14985415]

19. Shibuki K, et al. Dynamic imaging of somatosensory cortical activity in the rat visualized by flavoprotein autofluorescence. J Physiol. 2003; 549:919–927. [PubMed: 12730344]

20. Franklin, KBJ.; P.G.. The mouse brain in stereotaxic coordinates. Academic Press; San Diego, CA: 2008.

21. Spreafico R, Barbaresi P, Weinberg RJ, Rustioni A. SII-projecting neurons in the rat thalamus: a single- and double-retrograde-tracing study. Somatosens Res. 1987; 4:359–375. [PubMed: 3589289]

22. Llano DA, Theyel BB, Mallik AK, Sherman SM, Issa NP. Rapid and Sensitive Mapping of Long-Range Connections In Vitro Using Flavoprotein Autofluorescence Imaging Combined With Laser Photostimulation. J Neurophysiol. 2009; 101:3325–3340. [PubMed: 19321634]

23. Groh A, de Kock CPJ, Wimmer VC, Sakmann B, Kuner T. Driver or Coincidence Detector: Modal Switch of a Corticothalamic Giant Synapse Controlled by Spontaneous Activity and Short-Term Depression. Journal of Neuroscience. 2008; 28:9652–9663. [PubMed: 18815251]

24. Diamond ME, Armstrong-James M, Budway MJ, Ebner FF. Somatic sensory responses in the rostral sector of the posterior group (POm) and in the ventral posterior medial nucleus (VPM) of the rat thalamus: dependence on the barrel field cortex. J Comp Neurol. 1992; 319:66–84. [PubMed: 1592906]

25. Mathers LH. The synaptic organization of the cortical projection to the pulvinar of the squirrel monkey. J Comp Neurol. 1972; 146:43–60. [PubMed: 4627260]

26. Guillery RW, Feig SL, Van Lieshout DP. Connections of higher order visual relays in the thalamus: a study of corticothalamic pathways in cats. J Comp Neurol. 2001; 438:66–85. [PubMed: 11503153]

27. Rouiller EM, Welker E. Morphology of corticothalamic terminals arising from the auditory cortex of the rat: a Phaseolus vulgaris-leucoagglutinin (PHA-L) tracing study. Hear Res. 1991; 56:179–190. [PubMed: 1769912]

28. Ojima H. Terminal Morphology and Distribution of Corticothalamic Fibers Originating from Layers 5 and 6 of Cat Primary Auditory Cortex. Cereb. Cortex. 1994; 4:646–663. [PubMed: 7703690]

29. Bajo VM, et al. Morphology and spatial distribution of corticothalamic terminals originating from the cat auditory cortex. Hear Res. 1995; 83:161–174. [PubMed: 7607982]

30. Jeffery A, Winer DTLCLH. Two systems of giant axon terminals in the cat medial geniculate body: Convergence of cortical and GABAergic inputs. The Journal of Comparative Neurology. 1999; 413:181–197. [PubMed: 10524332]

31. Hazama M, Kimura A, Donishi T, Sakoda T, Tamai Y. Topography of corticothalamic projections from the auditory cortex of the rat. Neuroscience. 2004; 124:655–667. [PubMed: 14980736]

32. Bender DB. Visual activation of neurons in the primate pulvinar depends on cortex but not colliculus. Brain Research. 1983; 279:258–261. [PubMed: 6640346]

33. Susan C, Van Horn SMS. Differences in projection patterns between large and small corticothalamic terminals. The Journal of Comparative Neurology. 2004; 475:406–415. [PubMed: 15221954]

34. Daniel A, Llano SMS. Evidence for nonreciprocal organization of the mouse auditory thalamocortical-corticothalamic projection systems. The Journal of Comparative Neurology. 2008; 507:1209–1227. [PubMed: 18181153]

35. Kato N. Cortico-thalamo-cortical projection between visual cortices. Brain Research. 1990; 509:150–152. [PubMed: 2306630]

36. Bourassa J, Desche & nes M. Corticothalamic projections from the primary visual cortex in rats: a single fiber study using biocytin as an anterograde tracer. Neuroscience. 1995; 66:253–263. [PubMed: 7477870]

37. Bourassa J, Pinault D, Deschenes M. Corticothalamic projections from the cortical barrel field to the somatosensory thalamus in rats: a single-fibre study using biocytin as an anterograde tracer. Eur J Neurosci. 1995; 7:19–30. [PubMed: 7711933]

38. Guillery RW. Branching Thalamic Afferents Link Action and Perception. J Neurophysiol. 2003; 90:539–548. [PubMed: 12904485]

39. Guillery RW, Sherman SM. The thalamus as a monitor of motor outputs. Philos Trans R Soc Lond B Biol Sci. 2002; 357:1809–1821. [PubMed: 12626014]

40. Lam Y-W, Sherman SM. Mapping by Laser Photostimulation of Connections Between the Thalamic Reticular and Ventral Posterior Lateral Nuclei in the Rat. J Neurophysiol. 2005; 94:2472–2483. [PubMed: 16160090]

41. Lam Y-W, Nelson CS, Sherman SM. Mapping of the Functional Interconnections Between Thalamic Reticular Neurons Using Photostimulation. J Neurophysiol. 2006; 96:2593–2600. [PubMed: 16855107]

42. Lam Y-W, Sherman SM. Different Topography of the Reticulothalmic Inputs to First- and Higher-Order Somatosensory Thalamic Relays Revealed Using Photostimulation. J Neurophysiol. 2007; 98:2903–2909. [PubMed: 17881481]

43. Shepherd GMG, Pologruto TA, Svoboda K. Circuit Analysis of Experience-Dependent Plasticity in the Developing Rat Barrel Cortex. Neuron. 2003; 38:277–289. [PubMed: 12718861]

44. Callaway EM, Katz LC. Photostimulation using caged glutamate reveals functional circuitry in living brain slices. Proceedings of the National Academy of Sciences of the United States of America. 1993; 90:7661–7665. [PubMed: 7689225]
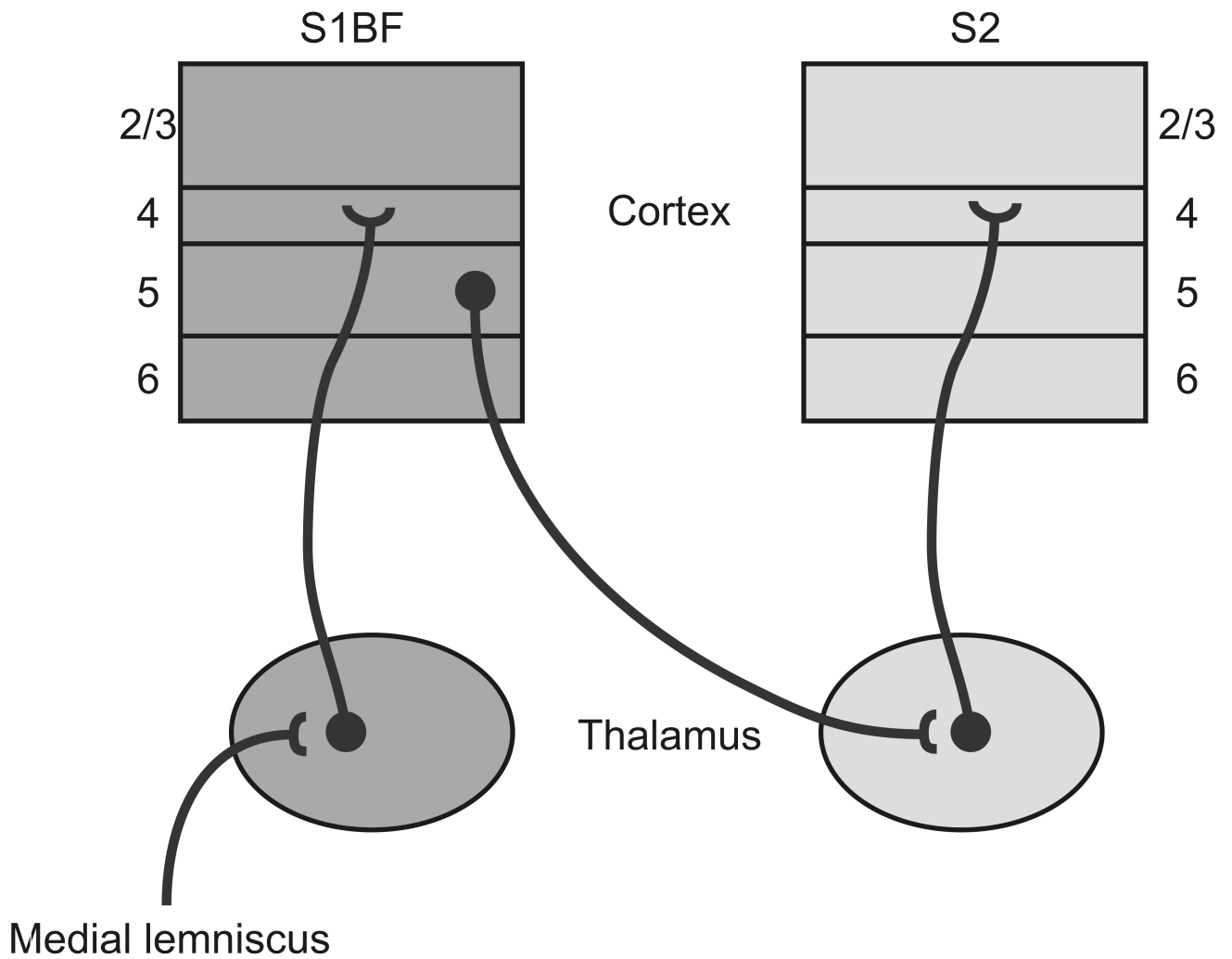
Figure 1.
Line drawing of the corticothalamocortical circuit. Red delineates the indirect, corticothalamocortical circuit; the direct corticocortical pathway is in grey. S1BF = barrel field of the primary somatosensory cortex, S2 = secondary somatosensory cortex, POm = posterior medial nucleus of the thalamus, VPm = ventroposteriomedial nucleus of the thalamus.
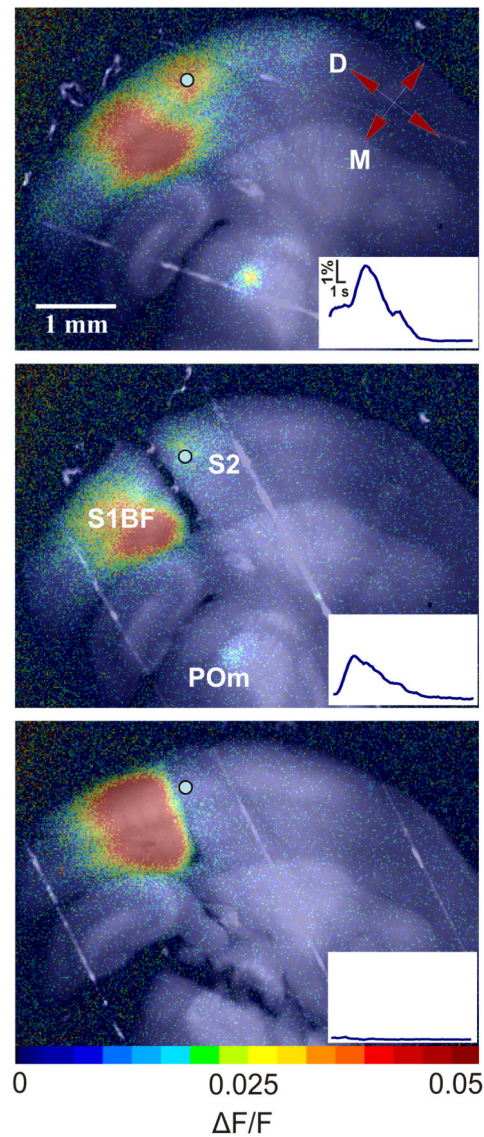
Figure 2.
Demonstration of corticothalamocortical pathway sufficiency to drive secondary somatosensory cortex activity: electrical stimulation. Panels are F/F (change in fluorescence/baseline fluorescence) images overlaid on top of raw images for anatomy. Insets are optical traces for the region delineated by the blue circles in secondary somatosensory cortex. Panels A–C depict a 'cut sequence' experiment. 1/1 experiments shown.

a.   Secondary somatosensory cortex response to S1BF stimulation in a somatosensory slice preparation.

b.   Secondary somatosensory cortex response following a cut between S1 and secondary somatosensory cortex. F/F decreased by 45.5% in secondary somatosensory cortex and 11.6% in POm compared to baseline (a).

c. Cortical response following thalamic ablation. See Supplementary Video 1 online. F/F decreased by 81.6% in secondary somatosensory cortex and 92.7% in POm compared to baseline (a).
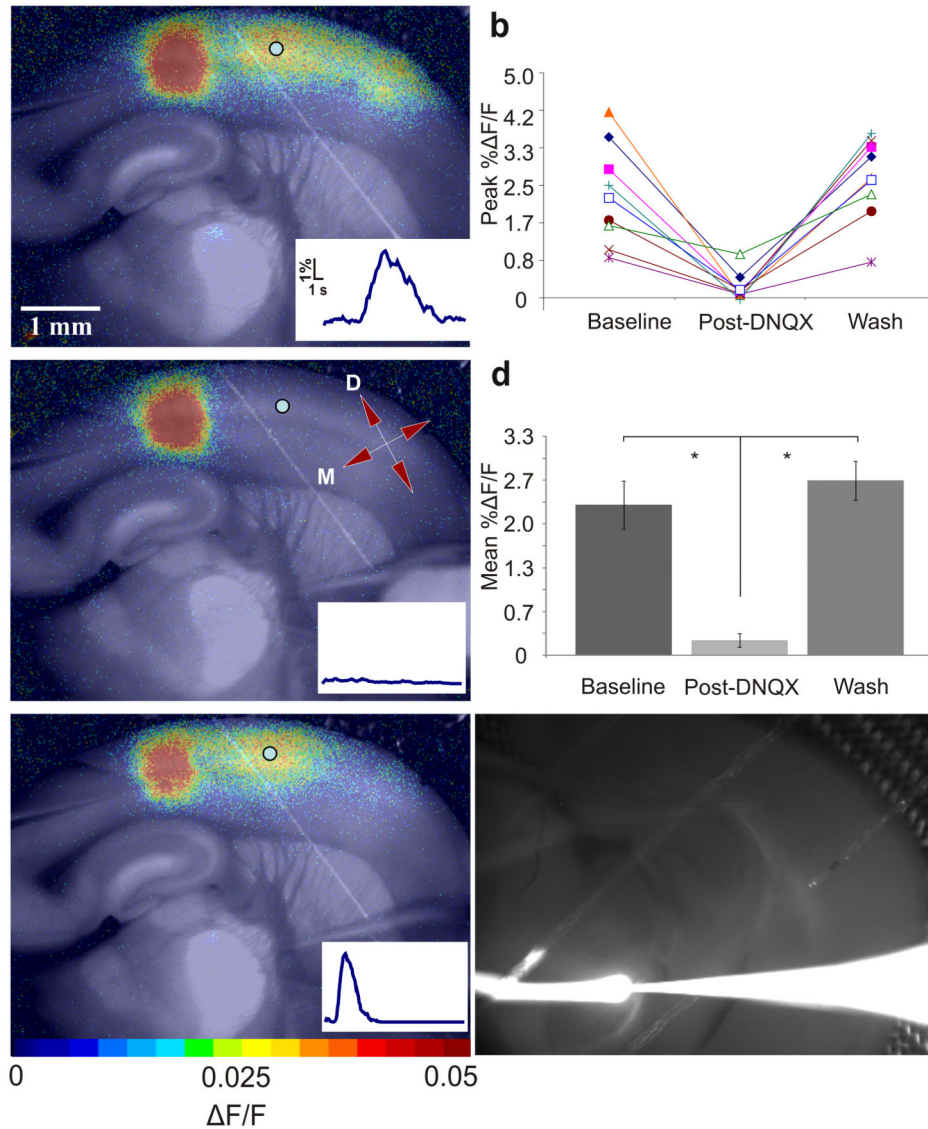
Figure 3.
Demonstration of corticothalamocortical pathway sufficiency to drive secondary somatosensory cortex activity: reversible inactivation. Panels a–c depict elimination of secondary somatosensory cortex response with AMPA receptor blockade in thalamus. 1/9 experiments shown.

a. Stimulation of layer 5B of S1BF via microspritzing of glutamate (see Methods).

b. Maximum percent ΔF/F before, during, and after DNQX – all Runs. 5×5 regions of interest were chosen in secondary somatosensory cortex for each trial. These regions were analyzed to determine maximal ΔF/F values during the baseline run (before DNQX), post-DNQX run and washout. Values for all nine experiments are plotted.

c. Slice response to the same stimulus as (a) ~4 minutes after local application of 500μM DNQX in the thalamic hotspot. Directional axis: D = dorsal, M = medial. In d, color bar corresponds to colors in panels.

d. Mean percent F/F before, during, and after DNQX inactivation of thalamus. The data shown in (b) were averaged and compared using a two-tailed t-test (an asterisk indicates a significant difference; see Results and Methods). Error bars indicate s.e.m. Means and standard errors were the following: 2.29 +/− 0.36% before DNQX, 0.2 +/− 0.10% Post-DNQX, 2.66+/− 0.30% Wash.

e. Response after DNQX washout. See Supplementary Video 2 online.

f. Injection spread control. We injected a fluorescent tracer into the thalamus using the same paradigm we used while injecting DNQX. The white line extending left from the electrode tip represents the tracer stream. ACSF flowed from right to left. See Supplementary Video 3 online.
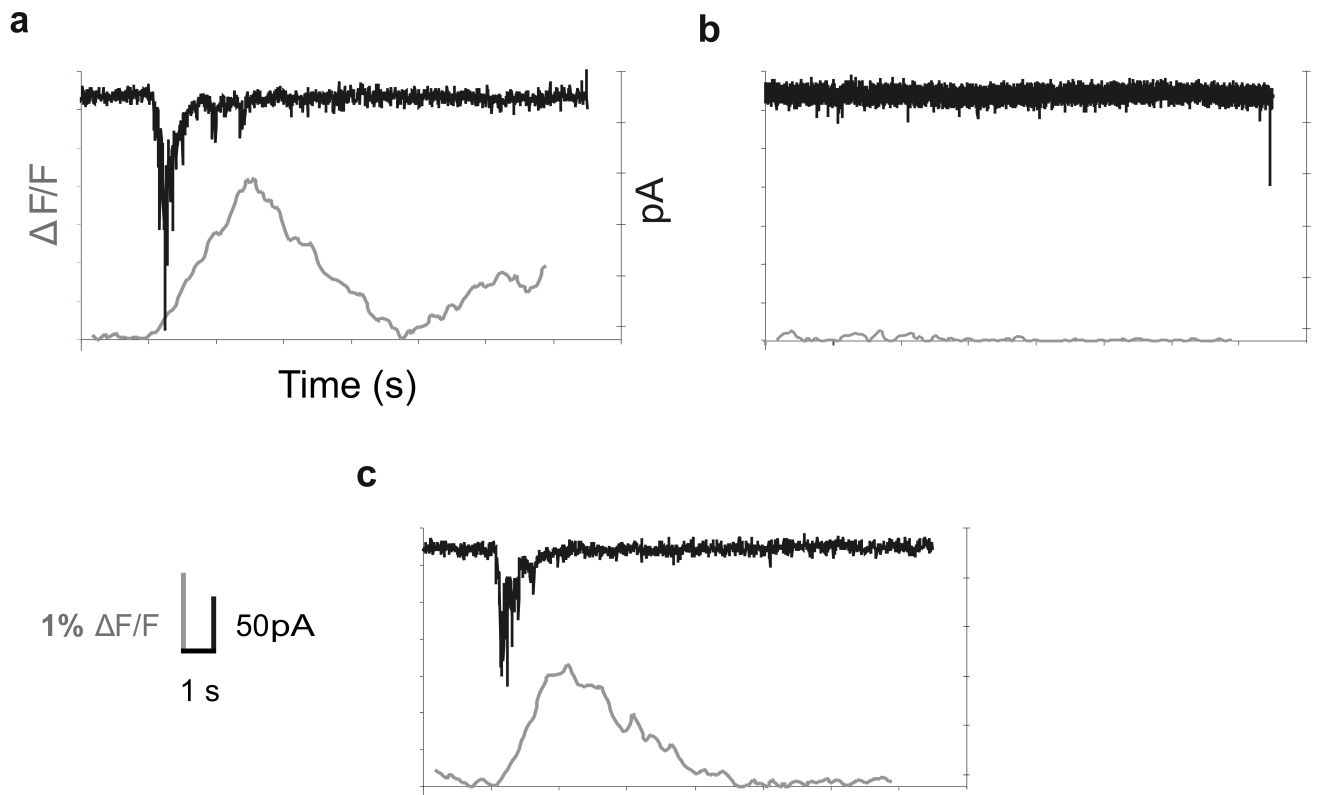
Figure 4.
Simultaneous flavoprotein autofluorescence imaging and whole-cell recording in secondary somatosensory cortex. Panels depict optical traces along with voltage clamp recordings from a representative (1/3) neuron in secondary somatosensory cortex before (a), ~6 minutes after (b) and ~12 minutes after (c) local DNQX application to thalamus. Optical traces and intracellular recordings were consistent (no cellular activity in conditions of no optical activity) and temporally synchronized at onset. See inset in lower left corner for scale.